Evaluating the effects of climate change on precipitation and temperature for Iran using RCP scenarios

Shahab Doulabian, Saeed Golian, Amirhossein Shadmehri Toosi and Conor Murphy

ABSTRACT

Climate change has caused many changes in hydrologic processes and climatic conditions globally, while extreme events are likely to occur more frequently at a global scale with continued warming. Given the importance of general circulation models (GCMs) as an essential tool for climate studies at global/regional scales, together with the wide range of GCMs available, selecting appropriate models is of great importance. In this study, six synoptic weather stations were selected as representative of different climatic zones over Iran. Utilizing monthly data for 20 years (1981–2000), the outputs of 25 GCMs for surface air temperature (SAT) and precipitation were evaluated for the historical period. The root-mean-square error and skill score were chosen to evaluate the performance of GCMs in capturing observed seasonal climate. Finally, the outputs of selected GCMs for the three Representative Concentration Pathways emission scenarios (RCPs), namely RCP2.6, RCP4.5, and RCP8.5, were downscaled using the change factor method for each station for the period 2046–2065. Results indicate that SAT in all months is likely to increase for each region, while for precipitation, large uncertainties emerge, despite the selection of climate models that best capture the observed seasonal cycle. These results highlight the importance of selecting a representative ensemble of GCMs for assessing future hydro-climatic changes for Iran.

Key words | climate change, GCMs, Iran, precipitation, RCPs, surface air temperature

Shahab Doulabian
Saeed Golian (corresponding author)
Department of Civil Engineering,
Shahrood University of Technology,
Shahrood, Semnan,
Iran
E-mail: *saeed.golian@mu.ie*

Saeed Golian
Conor Murphy
Irish Climate Analysis and Research UnitS (ICARUS), Department of Geography,
Maynooth University,
Maynooth,
Ireland

Amirhossein Shadmehri Toosi
Department of Civil Engineering,
Ferdowsi University of Mashhad,
Mashhad, Khorasan Razavi,
Iran

INTRODUCTION

Climate change (CC), driven by increases in greenhouse gases concentrations in the atmosphere, as a consequence of anthropogenic activities, has led to an increase in the global temperature of approximately 1 °C since the pre-industrial period (Dibike & Coulibaly 2005; Feng *et al.* 2014; Bekele *et al.* 2019). Moreover, CC can alter local climatic conditions and consequently accelerate hydrological processes (Kim *et al.* 2011; Thomas *et al.* 2018; Bekele *et al.* 2019). The integration of likely changes in hydrology is critically important for flood risk reduction and water resource management (Broderick *et al.* 2019; Toosi *et al.* 2019). Effective adaptation measures in these sectors require CC to be factored into an investment in long-lived infrastructure, upon which a society depends (Milly *et al.* 2008; Li *et al.* 2016; Taye *et al.* 2018; Bekele *et al.* 2019; Broderick *et al.* 2019). Several criteria determine the rainfall–runoff response, including the characteristics of the basin, vegetation density, soil type, basin shape and size, and antecedent moisture conditions (which vary seasonally and on an event basis), controlling the amount of rainfall that can permeate into the soil (Alaghmand *et al.* 2014; Jajarmizadeh *et al.* 2016; Toosi *et al.* 2019). Therefore, it is essential to

doi: 10.2166/wcc.2020.114

understand how hydrological processes are expected to change, together with the degree of uncertainty in the hydrological response at the regional scale (Dessu & Melesse 2013; Bekele *et al.* 2019).

General circulation models (GCMs) are the most widely used tools for investigating CC at global/regional scales through the production of climate scenarios for present and future time horizons. They have been found to be valuable tools for identifying hydrologic consequences of changes in the climate variables (Ullah *et al.* 2019; Thomas *et al.* 2018; Phillips *et al.* 2019; Warnatzsch & Reay 2019; Yang *et al.* 2019). The evaluation of global trends in GCM outputs has suggested that drier areas will likely become drier and wetter areas will likely become wetter, with a notable expansion in arid and semi-arid climates (Feng *et al.* 2014; WWAP 2018). Nevertheless, a comprehensive investigation of regional and seasonal impacts of CC in the future is needed, particularly at regional scales (Aloysius *et al.* 2016).

The results of previous research have revealed that simulated CC impacts in different regions are diverse and are highly dependent on the climate models and emission scenarios employed (Dibike & Coulibaly 2005; Feng *et al.* 2014; Fiseha *et al.* 2014; Cousino *et al.* 2015; Wu *et al.* 2015; Bekele *et al.* 2019). A case in point is the region of the Middle East where CC impacts vary significantly with each season and the 'wet gets wetter, dry gets drier' paradigm is not necessarily followed (Taye *et al.* 2018). Zarghami *et al.* (2011) assessed the impact of CC on temperature and precipitation for six synoptic stations in a case study using the HADCM3 model and three emission scenarios, A1B, A2, and B1 for the years 2020, 2055, and 2090. Their results showed that under the A2 scenario, a 2.3 °C rise in average annual temperature and a 3% reduction in annual precipitation are expected in the middle of this century. Zhao *et al.* (2014) pointed out that arid and semi-arid areas globally will likely experience a significant increase in surface air temperature (SAT) under various Representative Concentration Pathways (RCP), that wet regions will likely become wetter, and dry regions will likely become drier. However, the extent to which future CC will affect regional shifts is still uncertain and differs from region to region. Taye *et al.* (2018) evaluated the possible impact of CC on water availability for a basin in Ethiopia using three climate models from Coupled Models Inter-comparison Project phase 5 (CMIP5) for three future periods. Their results revealed that water shortages are expected to become more severe for some parts of the basin. Mirdashtvan *et al.* (2018) characterized the changes in climatic variables for the period 2011–2040 under different RCP scenarios and quantified the uncertainty in future projections linked with the downscaling methods for one of the most vulnerable basins in Iran; the 'Karaj-Jajrud' located in the South Alborz range. In comparison with the baseline period, all scenarios showed a consistent growth in SAT and a reduction in precipitation, while precipitation-series uncertainty was found to be more than the air temperature series.

Although previous studies provide essential information about potential CC impacts (Zarghami *et al.* 2011; Sabeerali *et al.* 2013; Hosseini *et al.* 2018; Mirdashtvan *et al.* 2018), our understanding of CC impact on the hydrological characteristics in Iran is lacking. In recent years, heavy rainfall events, flash floods, droughts, and extreme temperatures have been widely observed in Iran (Madani 2014; Rahimi *et al.* 2019; Toosi *et al.* 2019; Vaghefi *et al.* 2019). Given the variability of hydro-climatological conditions across the country, adopting a national (or regional) allowance for the realization of future climate may fail to address the actual emergent risk locally (Scussolini *et al.* 2016; Broderick *et al.* 2019). There is, therefore, a need to assess likely CC impacts for specific stations to help develop adaptation measures (Ullah *et al.* 2019). Furthermore, in Iran, most recent studies have used a limited number of GCMs, meaning that uncertainty in the results of these models has been neglected. Although the choice of suitable climate models, that can capture basic facets of Iranian climatology, is of considerable importance, few studies have aimed to assess climate models in this regard. The current study aims to evaluate the impacts of future CC on seasonal SAT and precipitation for distinct climatological regions in Iran using six long-term, high-quality synoptic weather stations. The specific objectives are (1) to assess the ability of 25 GCMs from the CMIP5 archive to capture the observed seasonal variability in each variable for different regions of Iran and (2) using selected GCMs, to investigate the impacts of CC on future precipitation and SAT under various RCP scenarios.

METHODS AND DATA

The flowchart of the methodology adopted is shown in Figure 1. Precipitation and temperature simulations from 25 GCMs from CMIP5 are compared with observed data from six stations for each season. Models that best capture the seasonal cycle are selected for further use. Using the change factor method, the outputs of GCMs were downscaled for the future period (2046–2065). Finally, the impacts of CC are discussed on a station by station basis.

Study area

Located in Western Asia, Iran has an area of 1,640,195 km^2, a population of 81 million inhabitants, and is the second major country in the Middle East. It lies between 24°N

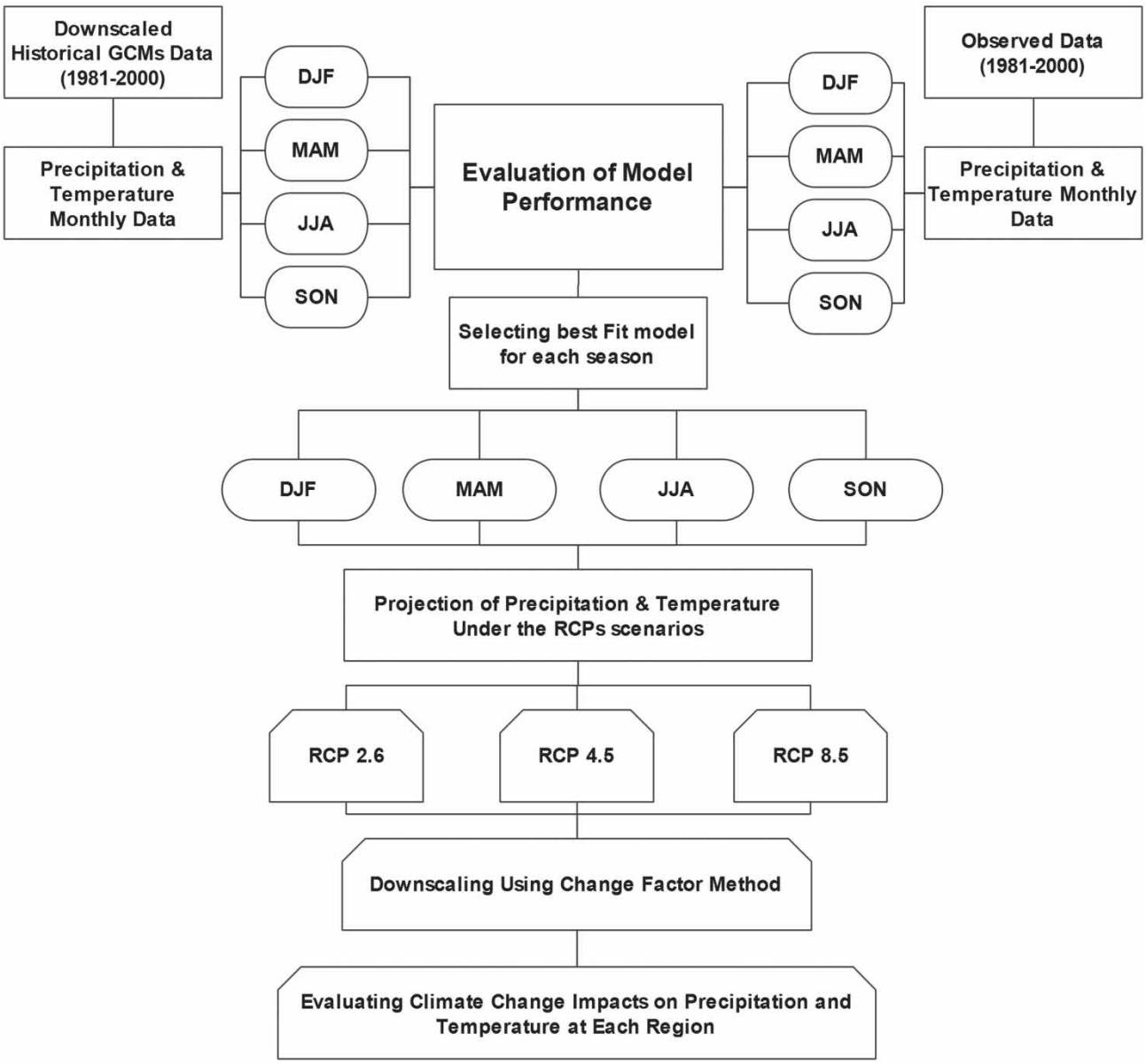

Figure 1 | Flowchart of the methodology employed (DJF: Winter; MAM: Spring; JJA: Summer; SON: Fall; RCP: Representative Concentration Pathway).

and 40°N latitude, and 44°E and 64°E longitude. Iran has diverse climates: mild and wet on the coast of the Caspian Sea, continental and arid in the plateau, cold in the high mountains, and dry and hot in the deserts of the southern coast and southeast. These distinct climate zones make it challenging to assess CC impacts in Iran and provide a stern test for climate models (Nicholson 2011; Mansouri *et al.* 2014). In this research, six synoptic stations were selected to be representative of specific climatic regimes (Figure 2). A description of the selected stations is presented in Table 1. Total monthly precipitation and mean monthly SAT data for these stations for the 20 years (1981–2000) were collected from the Iran Metrological Organization (IRIMO) (IRIMO 2016).

GCMs and CC scenarios

There are many factors to consider when selecting a model (Gleick 1986; Bekele *et al.* 2019; Gorguner *et al.* 2019). The purpose of the study and data availability are the dominant

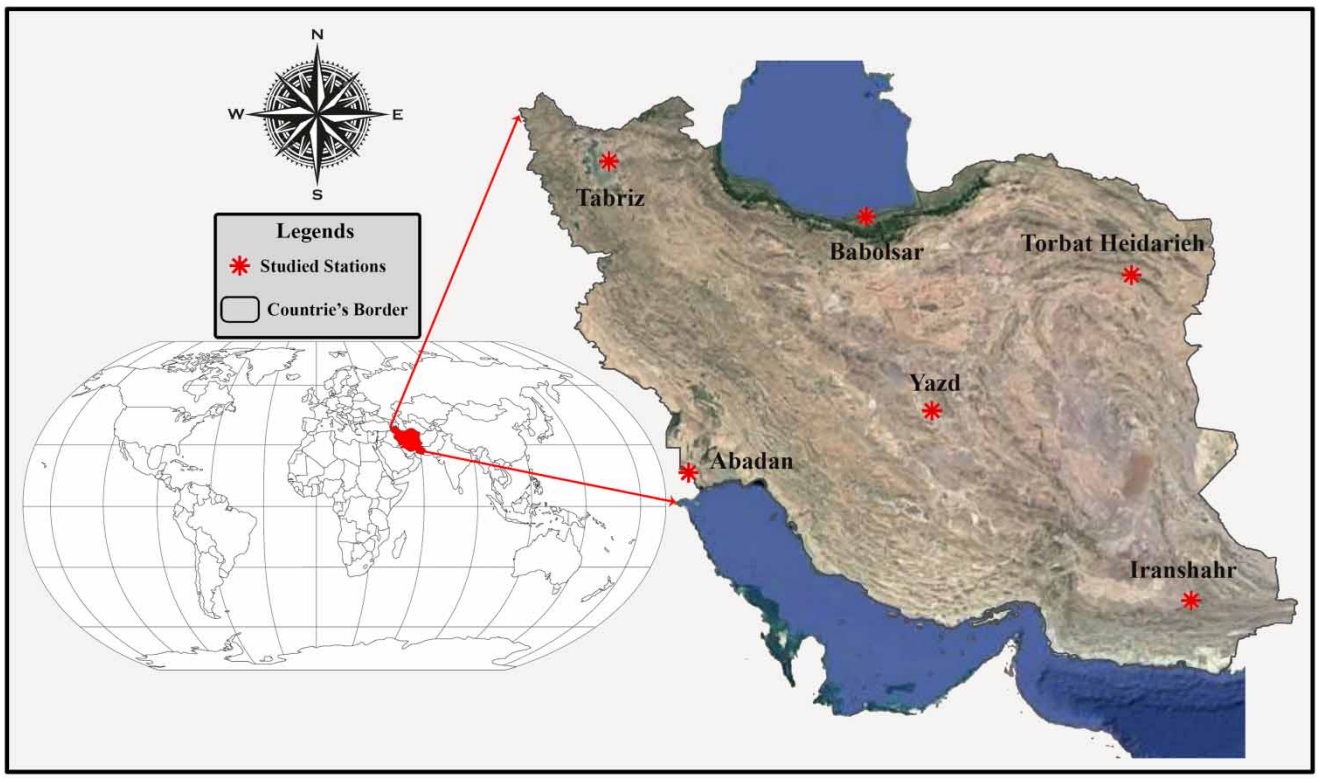

Figure 2 | Location of selected meteorological stations.

Table 1 | Description of synoptic stations used in the current study

Stations	Longitude (E)	Latitude (N)	Elevation (m)	Rainfall (mm)	Temperature (°C)	Climate
Abadan	48° 15′	30° 22′	6.6	164.8	26	Warm and desert
Babolsar	52° 39′	36° 43′	−21	932.3	16.9	Temperate and humid
Iranshahr	60° 42′	27° 12′	591.1	122.8	27	Dry and warm
Tabriz	46° 17′	38° 05′	1,361	262.2	12.2	Cold and mountainous
Torbat Heidarieh	59° 13′	35° 16′	1,450.8	283.8	14	Semi-arid and semi-desert
Yazd	54° 17′	31° 54′	1,273.2	60.4	19.3	Dry and warm

factors responsible for the choice of a particular model (Thomas *et al.* 2018). The most important base for obtaining CMIP5 data is ESGF, which is also the official website of the Intergovernmental Panel on Climate Change (IPCC). It provides users with the raw output from models for the historical period and future scenarios for a variety of time scales and a large number of climatic parameters such as temperature and precipitation. The main problem in using the output of GCMs is the low resolution of output grids which is too coarse to be useful for regional studies. Consequently, their outputs should be downscaled before being used in local studies. Given the importance of these models, some research centers have downscaled the output of GCMs to smaller grids and made the results accessible for all researchers worldwide. In the present study, the output from CMIP5 GCMs with $0.5^\circ \times 0.5^\circ$ grid size (downscaled using a bias-corrected statistical downscaling (BCSD) method) was used. Data were downloaded from http://gdo-dcp.ucllnl.org. Among available downscaled GCMs, 25 models which had projected climate under three RCP scenarios (RCP2.6, RCP4.5, and RCP8.5) were selected. These scenarios describe different climate futures according to the quantity of greenhouse gases emitted in the coming years (IPCC 2014).

RCPs explore credible future options by considering the uncertainties associated with future developments. RCP 2.6 is the most optimistic mitigation scenario, in which global annual greenhouse gas emissions peak to 440 ppm between 2010 and 2020 and then reduce considerably (van Vuuren *et al.* 2011). It implicates a global turnaround in environmental policies and collaborative actions from all emitters in the next few years for the active clearance of carbon dioxide from the atmosphere (van Vuuren *et al.* 2007). Under RCP 4.5, which is a stabilization scenario, emissions peak around 2040 then decrease and total radiative forcing reaching 540 ppm by 2100 before leveling off (Clarke *et al.* 2007; Thomson *et al.* 2011). RCP 8.5 is a pessimistic scenario in which emissions rise steadily over the 21st century, reaching 940 ppm by 2100, and continue increasing for another 100 years (Riahi *et al.* 2007) (Figure 3).

We used monthly values of total precipitation and average SAT for the historical (1981–2000) and future (2046–2065) periods. Table 2 shows the summary characteristics of the GCMs used in the current study.

Evaluation of model performance

Annual evaluation

The Taylor diagram has become a useful tool in the evaluation of the overall performance of climate models (Kim *et al.* 2014; Loikith *et al.* 2015; Warnatzsch & Reay 2019). The annual performance of models was assessed statistically using the Taylor diagram (Taylor 2001). It provides a brief statistical analysis of the degree of pattern correspondence between the modeled and observed data in terms of their

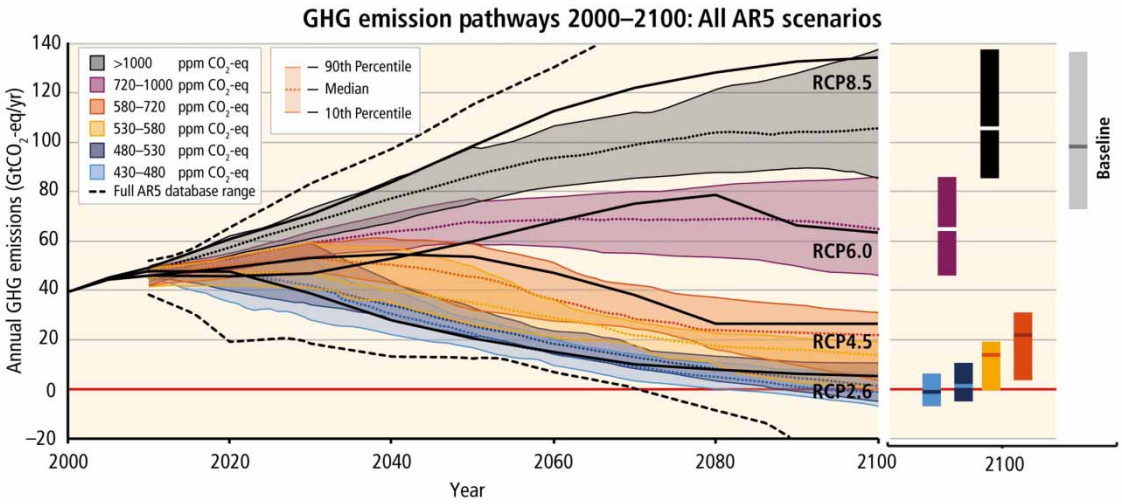

Figure 3 | Annual greenhouse emissions for different RCP scenarios (IPCC Fifth Assessment Report).

Table 2 | Characteristics of the 25 CMIP5 GCMs

No	Model identifier	Institution (Modeling Center)	Spatial resolution
1	bcc-csm1-1	Beijing Climate Center, China Meteorological Administration (BCC)	2.81 × 2.79
2	BNU-ESM	College of Global Change and Earth System Science, Beijing Normal University (GCESS)	2.81 × 2.79
3	CanESM2	Canadian Centre for Climate Modeling and Analysis, Canada (CCCma)	2.81 × 2.79
4	CCSM4	National Center for Atmospheric Research, USA (NCAR)	1.25 × 0.9
5	CESM1-CAM5	National Scince Foundation, Department of Energy, NCAR, USA (NSF-DOE-NCAR)	1.25 × 0.9
6	CNRM-CM5	Centre National de Researches Meteorologiques, Meteo-France (CNRM-CERFACS)	1.41 × 1.4
7	CSIRO-Mk3-6-0	Commonwealth Scientific and Industrial Research Organization (CSIRO-QCCCE)	1.875 × 1.86
8	EC-EARTH	EC-EARTH consortium (EC-EARTH)	1.125 × 1.12
9	FGOALS-g2	LASG, Institute of Atmospheric Physics, Chinese Academy of Sciences; and CESS, Tsinghua University (LASG-IAP)	2.81 × 2.79
10	FIO-ESM	The First Institute of Oceanography, SOA, China (FIO)	2.8 × 2.8
11	GFDL-CM3	NOAA Geophysical Fluid Dynamics Laboratory, USA (NOAA GFDL)	2.5 × 2
12	GFDL-ESM2G		
13	GFDL-ESM2M		
14	GISS-E2-R	NASA Goddard Institute for Space Studies (NASA GISS)	2.5 × 2
15	HadGEM2-AO	Met Office Hadley Centre (MOHC)	1.875 × 1.25
16	HadGEM2-ES	Instituto Nacional de Pesquisas Espaciais (INPE)	1.875 × 1.25
17	IPSL-CM5A-LR	Institute Pierre-Simon Laplace, France (IPSL)	3.75 × 1.875
18	IPSL-CM5A-MR		2.5 × 1.25
19	MIROC5	Atmosphere and Ocean Research Institute (The University of Tokyo), National Institute for Environmental Studies and Japan Agency for Marine-Earth Science and Technology (MIROC)	1.41 × 1.39
20	MIROC-ESM		2.81 × 1.77
21	MIROC-ESM-CHEM		
22	MPI-ESM-LR	Max Planck Institute for Meteorology, Germany (MPI-M)	1.875 × 1.85
23	MPI-ESM-MR		
24	MRI-CGCM3	Meteorological Research Institute, Japan (MRI)	1.125 × 1.125
25	NorESM1-M	Norwegian Climate Centre (NCC)	2.5 × 1.895

The expansions of the model identifiers can be found in http://www.ametsoc.org/Pubsacronymlist.

Pearson's correlation, root-mean-square error (RMSE), and the ratio of their variances which are simultaneously indicated by a single point on the plot (Taylor 2001). The diagram is particularly useful in assessing the relative merits of competing models and monitoring the overall performance of a model as it evolves.

Seasonal evaluation

Although the annual analysis illustrates a good overall picture of models' performance, the results can vary significantly in other temporal scales (e.g. seasonal). Therefore, the seasonal performance of the precipitation and SAT for all selected GCMs was examined using the RMSE and skill score (SS), and the best models were selected based on their seasonal performance. RMSE is always non-negative, and a value of 0 would indicate a perfect fit to the data. The SS index is used to evaluate the goodness of fit of a model prediction. It ranges from $-\infty$ to 1 with $SS = 1$ reflecting the perfect match of simulated and observed data, and $SS = 0$ shows that the model predictions are as accurate as of the mean of the observed data.

RMSE and SS are defined as follows:

$$\mathrm{RMSE} = \sqrt{\frac{\sum_{i=1}^{N}(m_i - o_i)^2}{N}} \quad (1)$$

$$\mathrm{SS} = 1 - \frac{\sum_{i=1}^{N}(m_i - o_i)^2}{\sum_{i=1}^{N}(\bar{o} - o_i)^2} \quad (2)$$

where m, o, and $\bar{o}$ are simulated, observed, and mean of the observed variable, respectively, and N is the number of observations (Murphy 1988; Pierce *et al.* 2009; Yang *et al.* 2019). Statistical evaluation of GCMs was performed using an observational dataset on a seasonal scale. RMSE and SS of the time-averaged model output were used for each station. In order to choose the top models, we divided each year into four seasons according to climate similarity, i.e. DJF, MAM, JJA, and SON represented winter, spring, summer, and fall, respectively (Fallah *et al.* 2017). Accordingly, the performance of models on the historical period was evaluated for each station, and models were selected as representative of each season for each station individually.

Future projections and downscaling

Several papers have previously indicated that the direct application of GCMs is limited due to their coarse resolution and systematic bias (Park *et al.* 2016; Yang *et al.* 2019). The coarse resolution prevents the models from sufficiently representing regional climatic processes. The biases potentially grow when used for CC simulations under global warming conditions. Bias correction should be applied to each model (Christensen *et al.* 2008; Yang *et al.* 2019). Downscaling is one of the approaches where GCM outputs are interpolated to meet local scale requirements and reduce bias (Mujumdar & Nagesh Kumar 2012; Raju & Kumar 2018). The change factor method is the most straightforward technique and is suitable for downscaling the mean value of climatic variables. In this study, to capture higher-resolution features and preserve the monthly variability of stationary observed data, the bias-correction change factor technique was applied to $0.5^\circ \times 0.5^\circ$ gridded GCMs to map the projections to weather stations' scale (Hansen *et al.* 2017; Ciscar *et al.* 2019).

The change factor method can be applied using Equations (3) and (4) (Anandhi *et al.* 2011; Yang *et al.* 2019) to ensure that the mean of downscaled data is quite close to those of the observations. Applying these equations, climatological precipitation and SAT data were downscaled to the desired regional scale (station point) during the projected period of 2046–2065, while the period 1981–2000 was used as the historical reference period.

$$P_{\mathrm{downscaling\ (m)}} = \overline{P_{\mathrm{obs_m}}} \times \left(\frac{\overline{P_{\mathrm{fut}}}}{\overline{P_{\mathrm{his}}}}\right)_{\mathrm{m}} \qquad \mathrm{m} = 1, \ldots, 12 \quad (3)$$

$$T_{\mathrm{downscaling\ (m)}} = \overline{T_{\mathrm{obs_m}}} + (\overline{T_{\mathrm{fut}}} - \overline{T_{\mathrm{his}}})_{\mathrm{m}} \qquad \mathrm{m} = 1, \ldots, 12 \quad (4)$$

where P and T indicate the precipitation and SAT, respectively. 'Obs' is the observational data, 'fut' is the projected raw data from a climate model (2046–2065), 'his' is the raw data from a climate model in the baseline period (1981–2000), and m is the month from January to December. The bar indicates the mean value (Yang *et al.* 2019).

RESULTS

Precipitation

We used the Taylor diagram to evaluate the overall performance of GCMs for annual precipitation. Figure 4 illustrates the performance of models for each station. The radial distance from the REF point, which is the indicator of observed values, is the centered pattern root-mean-square deviation (CRMSD), and the radial distance from the origin is the standard deviation, while the angle shows the correlation coefficient. Seasonal Taylor diagrams are presented in Figure S1 in the Supplementary section.

As illustrated in Figure 4, some models perform better than others; however, their overall performance is similar. The performance of the CMIP5 models for the Babolsar station is weaker, but all other stations illustrate the correlation value above 0.7. At the seasonal time scale, the performance of the simulated data for the historical period varied significantly (Figure S1), which highlights the importance of using seasonal data in choosing an appropriate

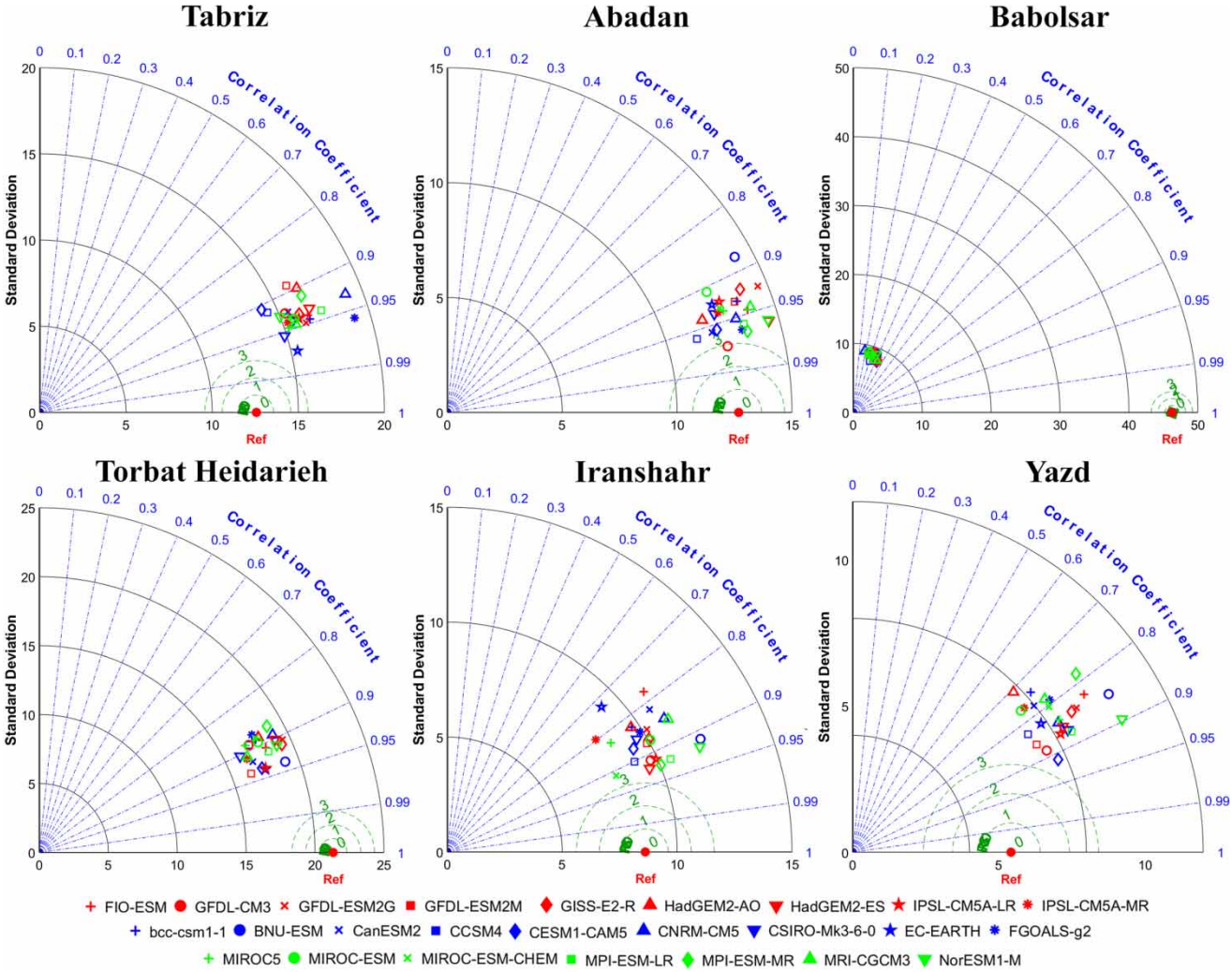

Figure 4 | Taylor diagrams for annual precipitation for each of the six stations. Simulation are derived from the CMIP5 models for the period 1981–2000.

model (Sabeerali *et al.* 2013; Li & Mao 2016). The acceptable performance of GCM models at the annual time scale cannot guarantee a good performance at monthly or seasonal time scales.

In Figure 5, boxplots depict the average range of seasonal results obtained from GCMs and red points show the average observation values. As can be seen, almost all models struggle to simulate the seasonal mean precipitation. This is particularly the case for the Babolsar station, where the model's results have a significant deviation from the observed values. For some stations, models tend to overestimate the seasonal precipitation, for example, Tabriz and Yazd in all seasons. However, model biases in different seasons vary considerably; for example in the Yazd station where biases in JJA and SON are relatively small, they are higher for MAM and DJF. Conversely, at the Babolsar station, all models underestimate seasonal precipitation. In particular, in DJF and SON, the model biases are considerably greater than in other seasons. The results for other stations were reasonably acceptable for all seasons, excluding for DJF at Torbat Heidarieh, JJA at Iranshahr, and SON at the Abadan station, where all models underestimated seasonal precipitation totals.

Model selection

The ranking of models based on SS is presented in Table 3. In this table, the relative values of RMSE are shown as the

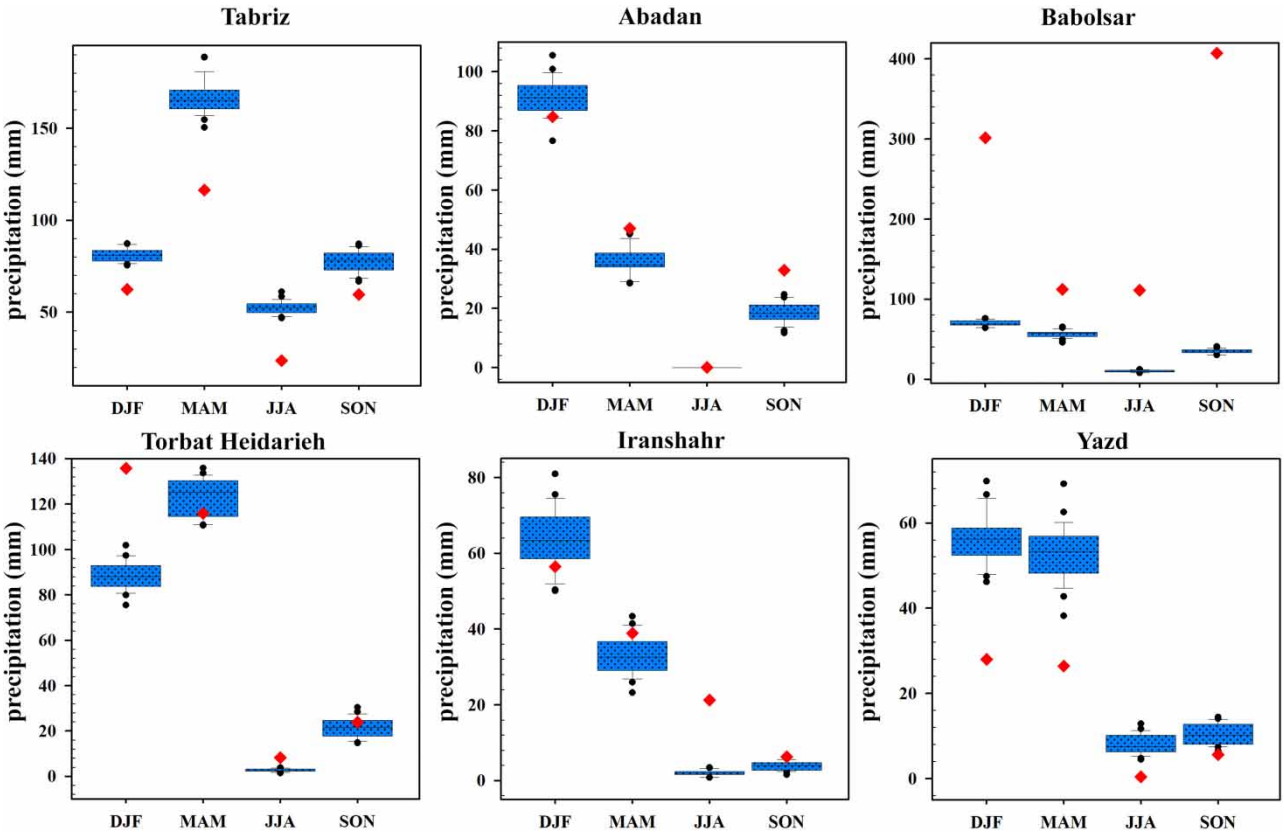

Figure 5 | Seasonal comparison of precipitation simulations from 25 CMIP5 simulations (box plots) with observed precipitation totals (red dot) from each of the six stations representing different regions of Iran for the years 1981–2000. Please refer to the online version of this paper to see this figure in colour: http://dx.doi.org/10.2166/wcc.2020.114.

Table 3 | Ranking from the GCM simulations of precipitation with respect to the observations for the 1981–2000 period using the SS score (in scale of 25)

	Abadan				Babolsar				Iranshahr				Tabriz				Torbat Heidarieh				Yazd			
	DJF	MAM	JJA	SON	DJF	MAM	JJA	SON	DJF	MAM	JJA	SON	DJF	MAM	JJA	SON	DJF	MAM	JJA	SON	DJF	MAM	JJA	SON
bcc-csm1-1	17	19	5	10	5	13	21	18	16	21	6	22	4	15	4	19	13	24	25	8	18	20	10	18
BNU-ESM	25	14	11	25	3	16	23	15	19	3	3	12	23	13	6	13	3	1	13	13	25	18	1	1
CanESM2	2	20	6	1	10	12	1	5	21	20	17	21	10	16	13	18	10	11	18	11	13	13	2	23
CCSM4	11	11	12	19	25	19	6	19	3	17	4	2	19	11	20	16	24	7	21	20	3	7	17	17
CESM1-CAM5	1	16	1	12	24	25	17	16	12	19	1	10	3	2	2	5	19	2	20	24	2	5	22	15
CNRM-CM5	8	6	10	18	20	2	25	20	20	7	15	25	22	24	24	2	11	20	19	12	11	15	18	16
CSIRO-Mk3-6-0	12	21	13	9	21	20	16	12	8	22	14	23	1	3	8	11	23	6	7	15	19	4	5	12
EC-EARTH	14	22	14	20	1	18	5	14	24	25	16	20	25	6	7	22	7	8	11	16	17	1	20	7
FGOALS-g2	18	3	2	4	19	5	15	4	17	11	18	16	11	25	12	24	21	19	15	7	16	22	16	19
FIO-ESM	19	4	17	17	7	1	19	6	25	23	21	24	18	20	1	9	4	18	5	10	24	8	14	9
GFDL-CM3	4	5	21	7	23	22	14	3	6	4	11	9	17	9	18	23	18	14	16	22	5	17	19	22
GFDL-ESM2G	24	12	22	15	4	7	10	7	14	15	8	8	16	14	19	14	1	22	2	6	22	11	23	4
GFDL-ESM2M	15	18	9	14	6	17	8	24	10	14	9	19	21	18	21	4	14	9	10	23	9	2	24	2
GISS-E2-R	22	17	3	16	2	8	7	9	9	12	22	4	14	23	25	25	8	4	23	2	20	9	3	14
HadGEM2-AO	3	23	8	13	22	10	22	10	22	9	7	6	12	21	17	10	20	17	14	1	1	24	6	20
HadGEM2-ES	20	2	18	8	9	14	12	17	1	10	10	5	24	17	9	3	9	12	3	4	14	10	11	11
IPSL-CM5A-LR	9	9	20	24	12	21	24	22	2	5	24	18	5	12	3	7	6	5	22	21	12	3	8	3
IPSL-CM5A-MR	5	25	23	2	14	23	13	1	11	24	19	14	15	1	5	21	15	10	1	19	7	12	12	21
MIROC5	7	13	15	21	13	9	18	21	18	16	23	7	2	8	11	8	25	16	12	14	6	16	13	5
MIROC-ESM	16	24	16	22	8	15	11	23	13	13	25	15	8	7	23	1	5	25	9	17	8	6	7	6
MIROC-ESM-CHEM	6	15	25	23	15	11	20	25	4	18	13	17	13	10	15	6	17	23	8	3	4	21	9	8
MPI-ESM-LR	10	8	24	11	18	6	4	8	7	1	20	3	6	19	10	15	2	15	6	9	10	19	4	13
MPI-ESM-MR	13	7	19	3	11	4	2	11	5	2	5	13	20	22	16	12	22	13	24	25	15	25	21	24
MRI-CGCM3	21	10	4	5	17	24	9	13	23	6	2	11	7	5	14	17	16	21	17	18	21	14	25	25
NorESM1-M	23	1	7	6	16	3	3	2	15	8	12	1	9	4	22	20	12	3	4	5	23	23	15	10

The magnitude of the relative RMSEs is shown as colors. Please refer to the online version of this paper to see this figure in colour: http://dx.doi.org/10.2166/wcc.2020.114.

color spectrum in which darker colors represent better performance (smaller RMSE). It can be seen that RMSE and SS rankings of individual models are quite similar. Tables S1–S6 in the Supplementary section contain the value of the SS score for different GCMs as well as additional indices, which were calculated to support our findings.

For the Tabriz station, four models, including CSIRO-Mk3-6-0 for DJF, IPSL-CM5A-MR for MAM, FIO-ESM for JJA, and MIROC-ESM for SON, showed better performance in terms of simulating the seasonal mean precipitation, and these models were used to simulate future changes under the RCP2.6, RCP4.5, and RCP8.5 scenarios. Likewise, for the Abadan station, three models including CESM1-CAM5, NorESM1-M, and CanESM2 were selected. At the Babolsar station, four models were selected, including EC-EARTH, FIO-ESM, CanESM2, and IPSL-CM5A-MR, while for the Torbat Heidarieh station, four selections were made, including GFDL-ESM2G, IPSL-CM5A-MR, BNU-ESM, and HadGEM2-AO. At the Iranshahr station, the selected models include HadGEM2-ES, MPI-ESM-LR, CESM1-CAM5, and CSIRO-Mk3-6-0 and lastly for the Yazd station, three models were selected, including HadGEM2-AO, EC-EARTH, and BNU-ESM.

Future projections

The change factor downscaling technique was applied to six synoptic stations. The precipitation change factors were estimated for those grid cells containing the stations to produce future projections. The obtained change factor value for each selected model over the baseline period was applied for relevant months for the future period. The projected precipitation under all scenarios for the years 2046–2065 was calculated and is depicted in Figure 6. The results for different stations show different behavior under various scenarios. Overall, the average annual precipitation is simulated to increase under all scenarios compared to the baseline period for the Abadan and Yazd stations. Similarly, at the Tabriz station under RCP2.6 and RCP8.5, annual precipitation is expected to increase. In general, simulations show that precipitation is likely to increase for the western stations, while projected decreases are apparent for the eastern stations. It is also expected that the greatest increase in precipitation under all RCPs is likely for the Yazd station, while the highest reduction occurs for the Iranshahr station, which has a dry and warm climate. Moreover, for the Iranshahr station, when the scenarios become more pessimistic, declines in precipitation are even greater.

The projection of seasonal precipitation changes under all emission scenarios is given in Table 4. The results show the greatest decrease (93% in JJA) under RCP4.5 at the Iranshahr station and the greatest increase (222% in JJA) under RCP8.5 at the Yazd station. The results of various scenarios show that there is not any specific pattern in precipitation change over different seasons but, for some stations, under all scenarios, the largest increase/decrease occurs in one season (e.g. for the Abadan and Iranshahr stations, the greatest decrease occurs in JJA). It is expected that in all stations, precipitation changes exhibit different behavior at different seasons when scenarios become more pessimistic.

Temperature

Similar to precipitation, we used the Taylor diagram to assess the overall performance of GCMs in the simulation of the annual SAT. Figure 7 shows the annual performance of models for all six stations. It can be seen that for all models, the results are almost the same, and their overall performance is very close. The correlation coefficient for all GCMs is above 0.95 in all stations. Corresponding Taylor diagrams of the seasonal cycle are summarized in Figure S2 of the Supplementary section.

From Figure 8, the performance of different models in capturing the seasonal temperature varied significantly across each station. While most GCMs give a reasonable prediction in terms of the mean SAT, at some stations, the models overestimated the seasonal SAT, e.g. in all seasons at the Babolsar station except DJF; in JJA and SON at the Abadan station, and all of the seasons except JJA at the Torbat Heidarieh station. Conversely, at the Iranshahr, Tabriz, and Yazd stations, all models underestimated the seasonal SAT. Overall, the model biases in the simulation of the SAT are relatively small for all stations.

Model selection

Similar to precipitation, we examined the ability of the GCMs to simulate the seasonal SAT. The same statistical

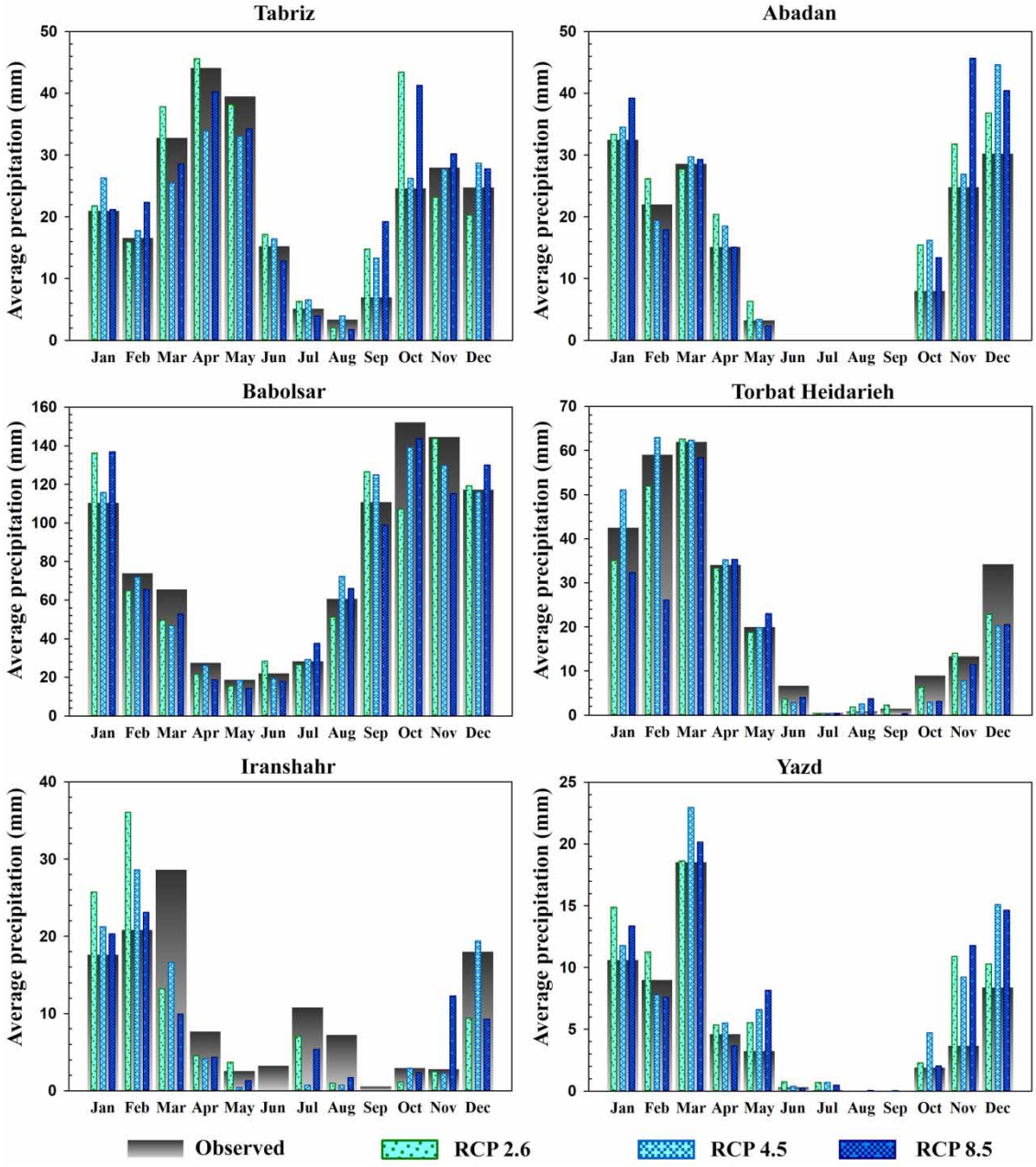

Figure 6 | Average observed (1981–2000) and simulated (2046–2065) monthly precipitation in different climatic zones of Iran for different CC scenarios.

indices, i.e. RMSE and SS, were used together to select GCMs with the best performance in the baseline period. The selected models were utilized to project future SAT changes at each station (Table 5). It is noteworthy that similar to precipitation, additional indices were also calculated for the SAT but were not used in model selection and are presented in the Supplementary section (Tables S7–S12).

For the Tabriz station, three models, i.e. CESM1-CAM5 for DJF and JJA, IPSL-CM5A-MR for MAM, and CanESM2 for SON were selected to examine future SAT changes under the RCP2.6, RCP4.5, and RCP8.5 scenarios. Likewise, for the Abadan station, four models including GISS-E2-R, IPSL-CM5A-MR, EC-EARTH, and GFDL-CM3 were selected. For the Babolsar station, three models including MPI-ESM-MR,

Table 4 | Precipitation changes (%) for the future period (2046–2065) in relation to the historical period (1981–2000)

	RCP2.6				RCP4.5				RCP8.5			
	DJF	MAM	JJA	SON	DJF	MAM	JJA	SON	DJF	MAM	JJA	SON
Abadan	14	16	−72	44	16	10	−52	31	15	−1	−25	80
Babolsar	6	−23	−4	−7	1	−19	9	−3	10	−24	9	−12
Iranshahr	26	−45	−62	−43	23	−46	−93	−18	−7	−60	−67	132
Tabriz	−7	4	7	37	17	−21	13	13	14	−12	−22	52
Torbat	−19	−1	−28	−5	−1	1	−30	−54	−42	1	−2	−38
Yazd	30	12	222	135	24	33	143	150	27	21	65	147

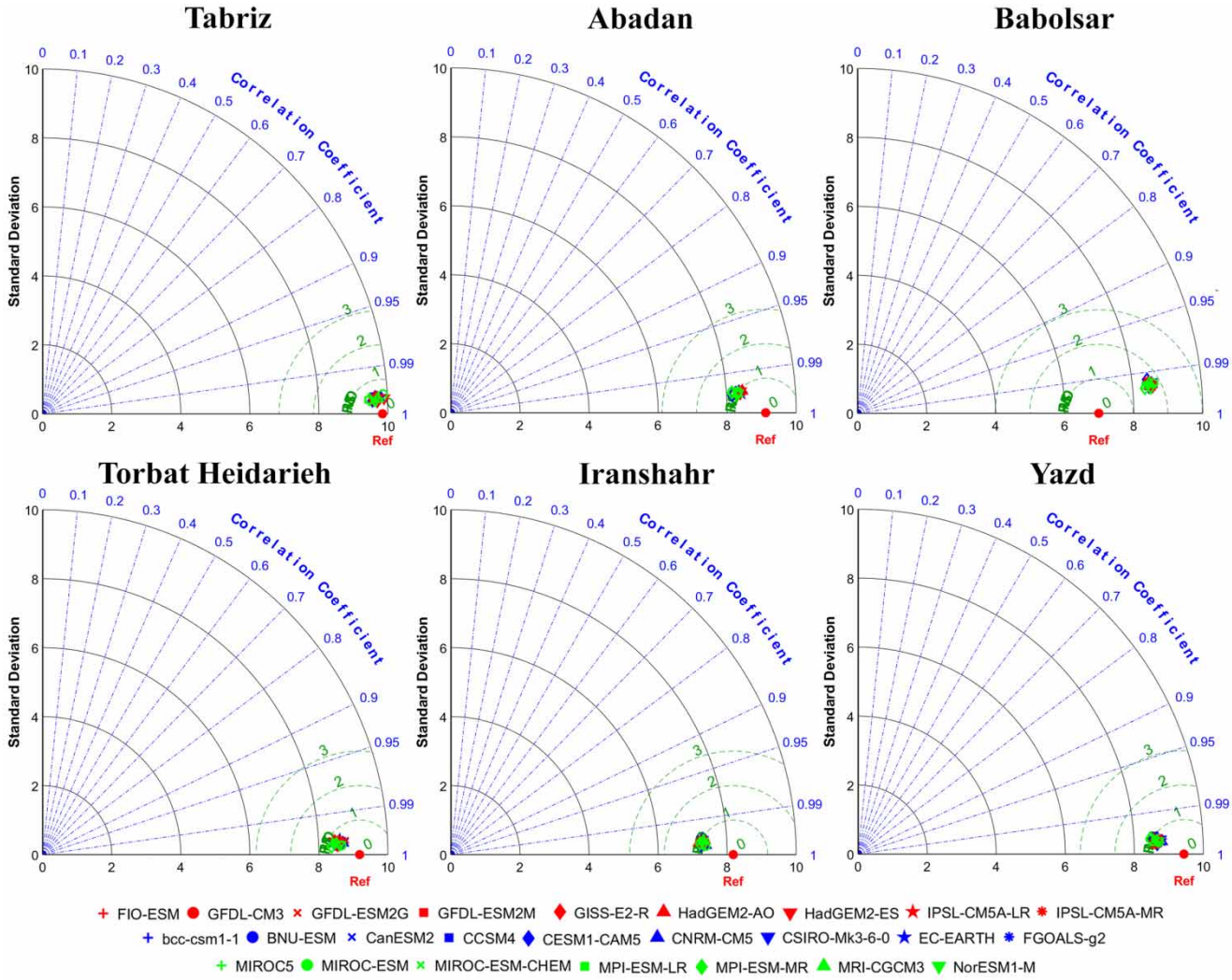

Figure 7 | Taylor diagram of the annual cycle of SAT; simulated in the CMIP5 models during 1981–2000.

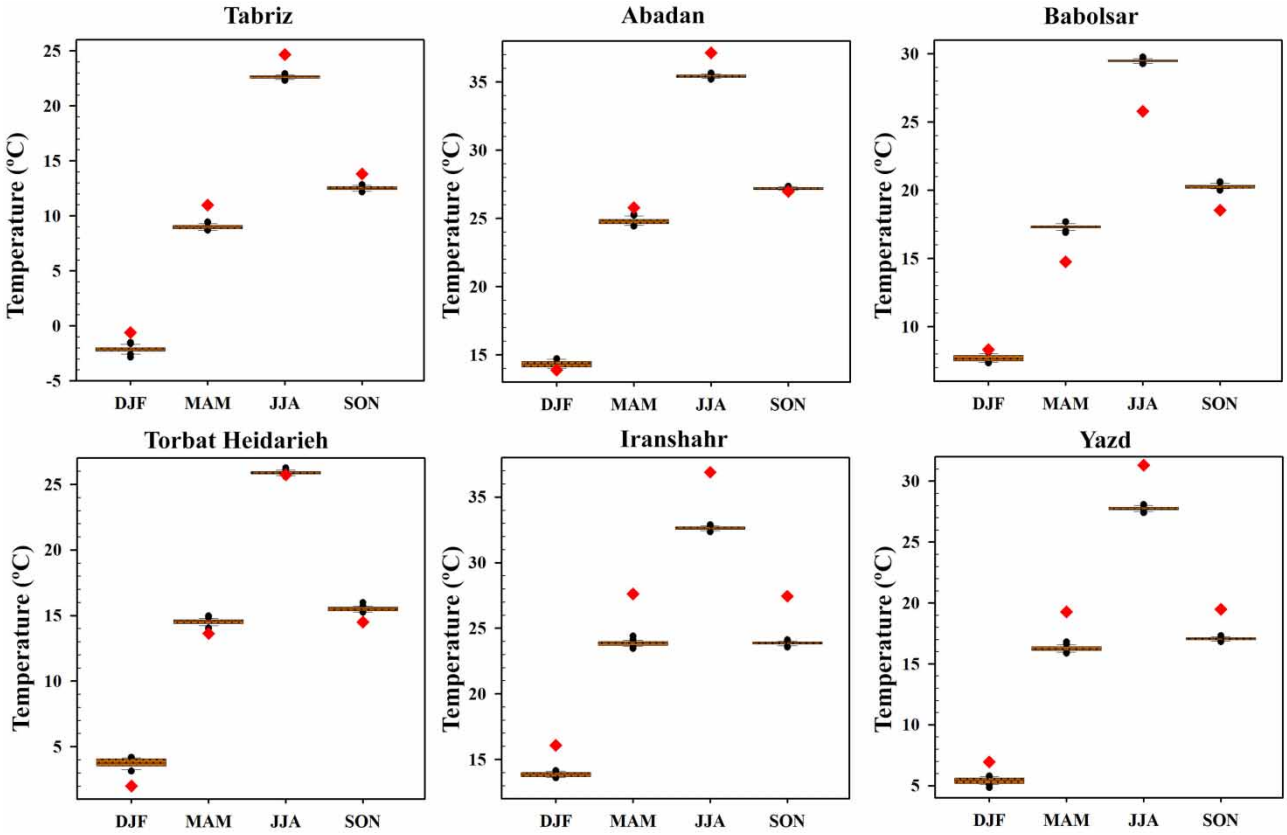

Figure 8 | Results of 25 CMIP5 climate models' SAT by seasonally comparing the observed and simulated data for the years 1981–2000.

Table 5 | Ranking from the GCMs simulations for SAT with respect to the observation for the 1981–2000 using the SS score

	Abadan				Babolsar				Iranshahr				Tabriz				Torbat Heidarieh				Yazd			
	DJF	MAM	JJA	SON	DJF	MAM	JJA	SON	DJF	MAM	JJA	SON	DJF	MAM	JJA	SON	DJF	MAM	JJA	SON	DJF	MAM	JJA	SON
bcc-csm1-1	19	19	6	22	2	16	25	25	7	24	4	2	5	15	4	12	21	11	25	25	10	20	1	1
BNU-ESM	23	10	10	25	19	22	17	24	6	10	5	1	11	6	12	2	22	16	16	23	1	10	9	2
CanESM2	11	8	3	20	17	15	23	22	11	4	1	4	17	7	3	1	14	17	21	19	11	6	2	3
CCSM4	12	12	11	16	9	19	20	9	25	11	21	25	8	11	9	23	7	22	18	1	21	8	19	21
CESM1-CAM5	24	6	22	11	14	25	24	21	15	1	24	18	1	2	1	16	23	24	23	11	8	1	10	4
CNRM-CM5	7	21	18	5	16	5	16	7	23	7	14	7	18	18	18	13	1	15	1	9	25	18	21	22
CSIRO-Mk3-6-0	3	13	23	10	20	12	13	1	24	22	25	16	20	12	16	24	3	7	17	6	24	17	18	17
EC-EARTH	10	5	1	21	12	20	14	14	14	3	7	20	24	5	13	17	12	18	12	14	20	3	7	19
FGOALS-g2	14	25	2	3	4	4	22	12	1	18	12	6	6	24	5	14	24	12	24	7	5	21	6	12
FIO-ESM	8	9	7	14	10	6	21	16	20	9	6	9	19	10	8	9	8	14	15	18	17	11	8	18
GFDL-CM3	4	23	24	1	21	8	7	2	19	23	9	19	16	19	24	25	9	8	11	4	22	24	16	25
GFDL-ESM2G	6	24	21	8	15	3	4	19	22	19	18	10	21	25	23	21	2	1	10	17	19	23	14	10
GFDL-ESM2M	17	4	17	24	25	9	2	8	10	2	19	23	10	9	19	11	11	19	3	12	13	2	22	20
GISS-E2-R	1	20	25	7	23	1	3	3	17	25	23	22	23	22	25	22	4	2	9	5	23	25	25	24
HadGEM2-AO	2	14	16	12	6	13	19	13	4	20	22	15	12	21	21	15	16	4	13	2	9	22	20	14
HadGEM2-ES	5	22	19	4	24	2	5	6	12	17	16	21	25	23	20	18	16	4	13	2	18	16	15	23
IPSL-CM5A-LR	13	11	8	17	18	17	11	10	13	15	20	11	15	17	10	8	10	21	5	21	14	5	11	6
IPSL-CM5A-MR	16	1	4	23	7	24	15	20	3	5	11	3	9	1	6	6	13	25	22	22	7	4	13	9
MIROC5	21	2	5	9	13	21	12	11	5	14	3	5	7	3	7	4	25	10	20	13	3	9	4	11
MIROC-ESM	9	18	20	13	22	10	18	15	16	6	15	24	22	20	2	3	5	6	2	15	15	14	17	15
MIROC-ESM-CHEM	18	16	15	2	3	11	10	5	18	13	8	17	13	14	15	20	18	23	7	8	2	7	3	5
MPI-ESM-LR	22	17	14	19	8	14	6	17	8	8	2	8	2	13	17	5	19	20	19	20	4	12	5	7
MPI-ESM-MR	25	15	12	15	1	7	1	4	2	12	13	12	3	16	22	19	20	9	8	10	6	19	24	16
MRI-CGCM3	15	7	9	18	11	23	9	23	21	21	17	14	14	4	14	7	6	13	4	24	16	15	23	8
NorESM1-M	20	3	13	6	5	18	8	18	9	16	10	13	4	8	11	10	15	3	6	16	12	13	12	13

The magnitude of the relative RMSEs is shown as colors. Please refer to the online version of this paper to see this figure in colour: http://dx.doi.org/10.2166/wcc.2020.114.

GISS-E2-R, and CSIRO-Mk3-6-0 were identified, while for the Torbat Heidarieh station, three models including CNRM-CM5, GFDL-ESM2G, and CCSM4 were selected. For the Iranshahr station, four models including FGOALS-g2, CESM1-CAM5, CanESM2, and BNU-ESM were chosen, and lastly for the Yazd station, three models including BNU-ESM, CESM1-CAM5, and bcc-csm1-1 were selected.

Future projections

Again, the change factor method was used as the downscaling method over six grid points in Iran. The simulation of SAT under all RCP scenarios for the period 2046–2065 was made, with results presented in Figure 9. The results indicated a positive trend in SAT in all months over all

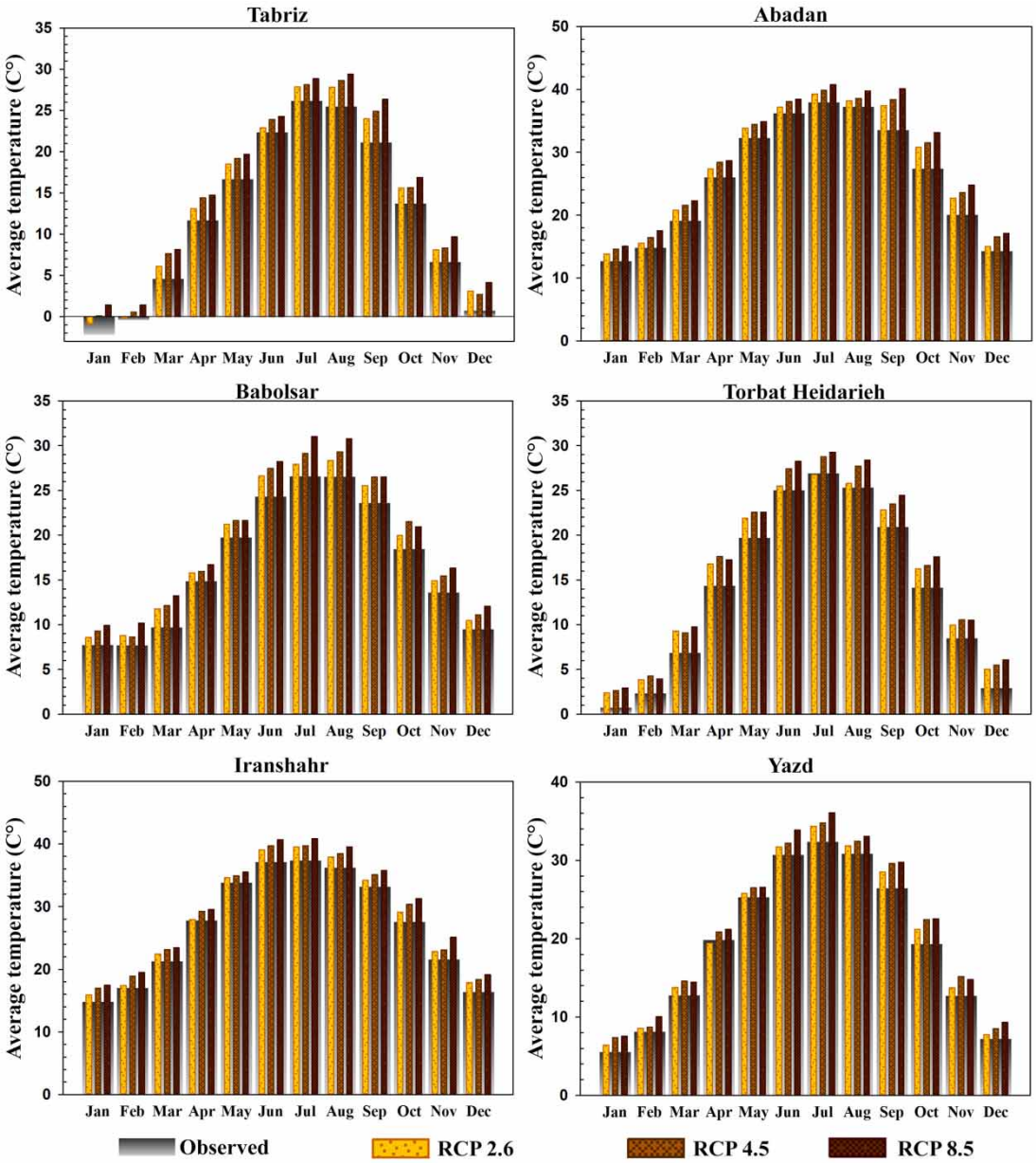

Figure 9 | Average observed (1981–2000) and simulated (2046–2065) monthly SAT in different climatic zones of Iran for different CC scenarios.

stations for the time period considered. The smallest and largest increases in SAT were derived under the RCP2.6 and RCP8.5 scenarios, respectively. For all six stations, there is an increase in the projected SAT, as the severity of the greenhouse scenario increases. The greatest increase in SAT under all RCPs is projected for the Abadan station, which has a warm and desert climate. For all stations, increases in SAT get larger as scenarios become more pessimistic.

Table 6 contains the seasonal projections of SAT changes over different stations under all RCP scenarios based on selected models. The results show the lowest increase (0.26 °C in JJA) under the RCP2.6 for the Torbat Heidarieh station and the highest increase (5.69 °C in SON) under RCP8.5 for the Abadan station.

DISCUSSION

CMIP3/CMIP5 simulations have long been used in various studies to assess the impacts of CC on humans and the environment. Many GCMs have been developed to represent future climate conditions at the global scale under different scenarios (Zhang *et al.* 2013; Mallakpour & Villarini 2015; Najafi & Moazami 2016; Ahmadalipour *et al.* 2017). Uncertainty is an indispensable part of GCM predictions which can be derived from their natural variability and coarse resolutions (Hawkins & Sutton 2011; Ahmadalipour *et al.* 2017). For that reason, selecting models that appropriately represents the regional-scale climate is an essential step before performing a regional CC impact assessment (Ahmadalipour *et al.* 2017). The better performance of the mean feature over the baseline period indicates the better simulations of the model (Sabeerali *et al.* 2013). Monthly datasets from CMIP5 can help researchers derive a more robust analysis and more reliable model comparison.

Evaluation of the results of the present study illustrates that models generally perform better in simulating SAT in comparison with precipitation. The majority of the models was unable to simulate the temporal pattern of precipitation at the seasonal scale in all stations. This is primarily due to the fact that the average rate of monthly variations in precipitation is higher in comparison to SAT (e.g. assume two following days, one with heavy rainfall and the other one with no rainfall (Ahmadalipour *et al.* 2017). Also, it can be attributed to the more stable nature of SAT which makes it easier to predict. Other research also confirms this issue (Samadi *et al.* 2013; Etemadi *et al.* 2014; Mirdashtvan *et al.* 2018).

Despite the fair simulation of GCMs in terms of the mean seasonal precipitation at most stations, all the models have difficulties in simulating precipitation at the Babolsar station, particularly in DJF and SON, where the models failed to simulate a reasonable correlation pattern with observations and underestimate totals during all seasons. Out of the 25 models analyzed, none gives a correlation of greater than 0.5 in simulation annual precipitation amounts at this station. Since GCMs produce results on the global scale (coarser resolution, Table 1), they tend to over/underestimate climatic variables on regional and global scales, failing to resolve the microscale climate (Ahmadalipour *et al.* 2017). However, the outcome of our study revealed that models with finer resolution do not always perform better than those with coarser resolutions (e.g. CCSM4, CNRM-CM5, MIROC5, and MRI-CGCM3).

Table 6 | SAT changes (°C) for the future period (2046–2065) relative to the historical period (1981–2000)

	RCP2.6				RCP4.5				RCP8.5			
	DJF	MAM	JJA	SON	DJF	MAM	JJA	SON	DJF	MAM	JJA	SON
Abadan	0.91	1.53	1.07	3.33	1.97	2.35	1.7	4.18	2.65	2.81	2.51	5.69
Babolsar	0.96	1.49	1.83	1.57	1.36	1.8	2.82	2.6	2.39	2.4	4.2	2.71
Iranshahr	0.99	0.7	1.93	1.26	2.01	1.48	2.39	2.08	2.61	1.86	3.45	3.25
Tabriz	1.3	1.58	1.52	2.06	1.73	2.76	2.22	2.45	2.93	3.21	2.85	3.8
Torbat	1.77	2.36	0.26	1.83	2.14	2.78	2.22	2.37	2.33	2.88	2.9	2.99
Yazd	0.62	0.38	1.35	1.65	1.25	1.36	1.82	2.91	2.03	1.45	3.03	2.87

Regarding other stations, some models provide realistic figures for some seasons in the baseline period. However, they failed to provide reasonable outputs for all seasons over the years.

At the Tabriz station, seasonal results show that the total mean precipitation under RCP8.5, which is a pessimistic scenario, increases in the future over wet seasons and decreases over dry seasons compared to the historical observations. These results agree with Zarghami *et al.* (2011) in the Northwest region of Iran, which were derived from the HADCM3 GCM model under the A2 scenario. Future simulations of SAT for most of the world show that there will be consistent warming in SAT with different magnitudes under all RCP scenarios (Mirdashtvan *et al.* 2018). SAT changes may have an impact on the hydrology of a region by increasing evapotranspiration rates even when no significant changes occur in precipitation amounts (Mirdashtvan *et al.* 2018). The results of this study on consistent warming in future periods are verified by the IPCC assessment reports, which state that the average SAT is rising globally (Samadi *et al.* 2013; Etemadi *et al.* 2014; IPCC 2014; Mirdashtvan *et al.* 2018).

It is noteworthy to mention that the selection of models in the current study is dependent on which metrics/skill scores you assess against. It means that if you were to look at how GCMs capture extremes or modes of variability that affect a region, you would most likely get a different set of climate models. Also, the models were chosen according to their seasonal performance, and there is no guarantee that this will remain the best model for other time scales. Therefore, there is a risk that uncertainties in future projections under-representing and should be considered in future studies. The question that arises here is that if the selected models for different seasons affect the physical integrity of the simulations. These models might be right for the wrong reasons or vice versa. This makes the future simulations lack internal consistency, which is suggested to be analyzed more in future works.

CONCLUSION

In this study, utilizing monthly data for 20 years (1981–2000), the outputs of 25 GCMs for SAT and precipitation were evaluated using observations for six synoptic stations over Iran. The performance of these models was evaluated using RMSE and SS, and the best models were selected at seasonal time scale and accordingly, the future data were generated. Although the annual performance of models was different, most models show an acceptable representation of the annual cycle of each variable at most stations. The GCM predictions at different time scales showed dissimilar uncertainties. Evaluation of the results of the present study illustrates that models generally perform better in simulating SAT compared to precipitation. The majority of the models was unable to simulate the temporal pattern of precipitation at seasonal scales at all stations. Therefore, there is less confidence in precipitation projections in comparison with SAT projections due to the unpredictable nature of the former. The results showed that the GCMs tend to over/underestimate climatic variables on regional and global scales, failing to resolve the microscale climate. Also, the results revealed that models with finer resolution do not always perform better than those with coarser resolutions. In most stations, some models provide realistic figures for some seasons in the baseline period. However, they failed to provide reasonable outputs for all seasons over the years. Overall, the results showed that the mean SAT is expected to increase in all seasons, while the precipitation change did not follow a specific trend. The outcomes of this study and related research can be a stimulus for the government to find new and sustainable adaptation strategies for the water sector.

ACKNOWLEDGEMENTS

We acknowledge the World Climate Research Programme's Working Group on Coupled Modelling, which is responsible for CMIP, and we thank the climate modeling groups (listed in Table 2 of this paper) for producing and making available their model output. For CMIP, the U.S. Department of Energy's Program for Climate Model Diagnosis and Intercomparison provides coordinating support and led the development of software infrastructure in partnership with the Global Organization for Earth System Science Portals. We would also like to thank the Downscaled CMIP3 and CMIP5 Climate and Hydrology Projections archives at

http://gdo-dcp.ucllnl.org/downscaled_cmip_projections/ for providing the BCSD CMIP5 downscaled data, as well as the re-gridded to 0.5° × 0.5° resolution GCMs data.

SUPPLEMENTARY MATERIAL

The Supplementary Material for this paper is available online at https://dx.doi.org/10.2166/wcc.2020.114.

REFERENCES

Ahmadalipour, A., Rana, A., Moradkhani, H. & Sharma, A. 2017 Multi-criteria evaluation of CMIP5 GCMs for climate change impact analysis. *Theoretical and Applied Climatology* **128** (1–2), 71–87.

Alaghmand, S., Beecham, S. & Hassanli, A. 2014 Impacts of vegetation cover on surface-groundwater flows and solute interactions in a semi-arid saline floodplain: a case study of the Lower Murray River, Australia. *Environmental Processes* **1** (1), 59–71.

Aloysius, N. R., Sheffield, J., Saiers, J. E., Li, H. & Wood, E. F. 2016 Evaluation of historical and future simulations of precipitation and temperature in central Africa from CMIP5 climate models. *Journal of Geophysical Research: Atmospheres* **121** (1), 130–152.

Anandhi, A., Frei, A., Pierson, D. C., Schneiderman, E. M., Zion, M. S., Lounsbury, D. & Matonse, A. H. 2011 Examination of change factor methodologies for climate change impact assessment. *Water Resources Research* **47** (3), W03501. doi:10.1029/2010WR009104.

Bekele, D., Alamirew, T., Kebede, A., Zeleke, G. & Melesse, A. M. 2019 Modeling climate change impact on the hydrology of Keleta watershed in the Awash River Basin, Ethiopia. *Environmental Modeling & Assessment* **24** (1), 95–107.

Broderick, C., Murphy, C., Wilby, R. L., Matthews, T., Prudhomme, C. & Adamson, M. 2019 Using a scenario-neutral framework to avoid potential maladaptation to future flood risk. *Water Resources Research* **55** (2), 1079–1104.

Christensen, J. H., Boberg, F., Christensen, O. B. & Lucas-Picher, P. 2008 On the need for bias correction of regional climate change projections of temperature and precipitation. *Geophysical Research Letters* **35** (20), L20709. doi:10.1029/2008GL035694.

Ciscar, J. C., Rising, J., Kopp, R. E. & Feyen, L. 2019 Assessing future climate change impacts in the EU and the USA: insights and lessons from two continental-scale projects. *Environmental Research Letters* **14** (8), 084010.

Clarke, L., Edmonds, J., Jacoby, H., Pitcher, H., Reilly, J. & Richels, R. 2007 *Scenarios of Greenhouse Gas Emissions and Atmospheric Concentrations*. University of Nebraska – Lincoln, U.S. Department of Energy Publications, p. 6.

Cousino, L. K., Becker, R. H. & Zmijewski, K. A. 2015 Modeling the effects of climate change on water, sediment, and nutrient yields from the Maumee River watershed. *Journal of Hydrology: Regional Studies* **4**, 762–775.

Dessu, S. B. & Melesse, A. M. 2013 Impact and uncertainties of climate change on the hydrology of the Mara River basin, Kenya/Tanzania. *Hydrological Processes* **27** (20), 2973–2986.

Dibike, Y. B. & Coulibaly, P. 2005 Hydrologic impact of climate change in the Saguenay watershed: comparison of downscaling methods and hydrologic models. *Journal of Hydrology* **307** (1–4), 145–163.

Etemadi, H., Samadi, S. & Sharifikia, M. 2014 Uncertainty analysis of statistical downscaling models using general circulation model over an international wetland. *Climate Dynamics* **42** (11–12), 2899–2920.

Fallah, B., Sodoudi, S., Russo, E., Kirchner, I. & Cubasch, U. 2017 Towards modeling the regional rainfall changes over Iran due to the climate forcing of the past 6000 years. *Quaternary International* **429**, 119–128.

Feng, S., Hu, Q., Huang, W., Ho, C. H., Li, R. & Tang, Z. 2014 Projected climate regime shift under future global warming from multi-model, multi-scenario CMIP5 simulations. *Global and Planetary Change* **112**, 41–52.

Fiseha, B. M., Setegn, S. G., Melesse, A. M., Volpi, E. & Fiori, A. 2014 Impact of climate change on the hydrology of upper Tiber River Basin using bias corrected regional climate model. *Water Resources Management* **28** (5), 1327–1343.

Gleick, P. H. 1986 Methods for evaluating the regional hydrologic impacts of global climatic changes. *Journal of Hydrology* **88** (1–2), 97–116.

Gorguner, M., Kavvas, M. L. & Ishida, K. 2019 Assessing the impacts of future climate change on the hydroclimatology of the Gediz Basin in Turkey by using dynamically downscaled CMIP5 projections. *Science of the Total Environment* **648**, 481–499.

Hansen, C. H., Goharian, E. & Burian, S. 2017 Downscaling precipitation for local-scale hydrologic modeling applications: comparison of traditional and combined change factor methodologies. *Journal of Hydrologic Engineering* **22** (9), 04017030.

Hawkins, E. & Sutton, R. 2011 The potential to narrow uncertainty in projections of regional precipitation change. *Climate Dynamics* **37** (1–2), 407–418.

Hosseini, R. H., Golian, S. & Yazdi, J. 2018 Evaluation of data-driven models to downscale rainfall parameters from global climate models outputs: the case study of Latyan watershed. *Journal of Water and Climate Change*, doi:10.2166/wcc.2018.191.

IPCC 2014 In: *Climate Change 2014: Synthesis Report. Contribution of Working Groups I, II and III to the Fifth Assessment Report of the Intergovernmental Panel on Climate Change* (Core Writing Team, R. K. Pachauri & L. A. Meyer, eds). IPCC, Geneva, Switzerland, p. 151.

IRIMO 2016 *Iran Metrological Organization*. Available from: https://www.irimo.ir.

Jajarmizadeh, M., Sidek, L. M., Mirzai, M., Alaghmand, S., Harun, S. & Majid, M. R. 2016 Prediction of surface flow by forcing of climate forecast system reanalysis data. *Water Resources Management* **30** (8), 2627–2640.

Kim, B. S., Kim, B. K. & Kwon, H. H. 2011 Assessment of the impact of climate change on the flow regime of the Han River basin using indicators of hydrologic alteration. *Hydrological Processes* **25** (5), 691–704.

Kim, J., Waliser, D. E., Mattmann, C. A., Goodale, C. E., Hart, A. F., Zimdars, P. A., Crichton, D. J., Jones, C., Nikulin, G., Hewitson, B. & Jack, C. 2014 Evaluation of the CORDEX-Africa multi-RCM hindcast: systematic model errors. *Climate Dynamics* **42** (5–6), 1189–1202.

Li, J. & Mao, J. 2016 Changes in the boreal summer intraseasonal oscillation projected by the CNRM-CM5 model under the RCP 8.5 scenario. *Climate Dynamics* **47** (12), 3713–3736.

Li, Y. L., Tao, H., Yao, J. & Zhang, Q. 2016 Application of a distributed catchment model to investigate hydrological impacts of climate change within Poyang Lake catchment (China). *Hydrology Research* **47** (S1), 120–135.

Loikith, P. C., Waliser, D. E., Lee, H., Kim, J., Neelin, J. D., Lintner, B. R., McGinnis, S., Mattmann, C. A. & Mearns, L. O. 2015 Surface temperature probability distributions in the NARCCAP hindcast experiment: evaluation methodology, metrics, and results. *Journal of Climate* **28** (3), 978–997.

Madani, K. 2014 Water management in Iran: what is causing the looming crisis? *Journal of Environmental Studies and Sciences* **4** (4), 315–328.

Mallakpour, I. & Villarini, G. 2015 The changing nature of flooding across the central United States. *Nature Climate Change* **5** (3), 250.

Mansouri, R., Ghanavati, E. & Servati, M. R. 2014 The assessment of geomorphological landscapes and geotourism potential role of the Ilam province with respect to sustainable development. *Journal of Geographical Data* **23** (90), 5–12 (in Persian).

Milly, P. C., Betancourt, J., Falkenmark, M., Hirsch, R. M., Kundzewicz, Z. W., Lettenmaier, D. P. & Stouffer, R. J. 2008 Stationarity is dead: whither water management? *Science* **319** (5863), 573–574.

Mirdashtvan, M., Najafinejad, A., Malekian, A. & Sa'doddin, A. 2018 Downscaling the contribution to uncertainty in climate-change assessments: representative concentration pathway (RCP) scenarios for the South Alborz Range, Iran. *Meteorological Applications* **25** (3), 414–422.

Mujumdar, P. & Nagesh Kumar, D. 2012 Hydrologic modeling for floods. In: *Floods in a Changing Climate: Hydrologic Modeling*. (International Hydrology Series). Cambridge University Press, Cambridge, UK, pp. 5–42.

Murphy, A. H. 1988 Skill scores based on the mean square error and their relationships to the correlation coefficient. *Monthly Weather Review* **116** (12), 2417–2424.

Najafi, M. R. & Moazami, S. 2016 Trends in total precipitation and magnitude–frequency of extreme precipitation in Iran, 1969–2009. *International Journal of Climatology* **36** (4), 1863–1872.

Nicholson, S. E. 2011 Asia. In: *Dryland Climatology*. Cambridge University Press, Cambridge, UK, pp. 351–373.

Park, C., Min, S. K., Lee, D., Cha, D. H., Suh, M. S., Kang, H. S., Hong, S. Y., Lee, D. K., Baek, H. J., Boo, K. O. & Kwon, W. T. 2016 Evaluation of multiple regional climate models for summer climate extremes over East Asia. *Climate Dynamics* **46** (7–8), 2469–2486.

Phillips, T. J., Bonfils, C. J. & Zhang, C. 2019 Model consensus projections of US regional hydroclimates under greenhouse warming. *Environmental Research Letters* **14** (1), 014005.

Pierce, D. W., Barnett, T. P., Santer, B. D. & Gleckler, P. J. 2009 Selecting global climate models for regional climate change studies. *Proceedings of the National Academy of Sciences* **106** (21), 8441–8446.

Rahimi, J., Malekian, A. & Khalili, A. 2019 Climate change impacts in Iran: assessing our current knowledge. *Theoretical and Applied Climatology* **135** (1–2), 545–564.

Raju, K. S. & Kumar, D. N. 2018 Downscaling techniques in climate modeling. In: *Impact of Climate Change on Water Resources*. Springer, Singapore, pp. 77–105.

Riahi, K., Grübler, A. & Nakicenovic, N. 2007 Scenarios of long-term socio-economic and environmental development under climate stabilization. *Technological Forecasting and Social Change* **74** (7), 887–935.

Sabeerali, C. T., Ramu Dandi, A., Dhakate, A., Salunke, K., Mahapatra, S. & Rao, S. A. 2013 Simulation of boreal summer intraseasonal oscillations in the latest CMIP5 coupled GCMs. *Journal of Geophysical Research: Atmospheres* **118** (10), 4401–4420.

Samadi, S., Wilson, C. A. & Moradkhani, H. 2013 Uncertainty analysis of statistical downscaling models using Hadley Centre Coupled Model. *Theoretical and Applied Climatology* **114** (3–4), 673–690.

Scussolini, P., Aerts, J. C., Jongman, B., Bouwer, L. M., Winsemius, H. C., de Moel, H. & Ward, P. J. 2016 FLOPROS: an evolving global database of flood protection standards. *Natural Hazards and Earth System Sciences* **16** (5), 1049–1061.

Taye, M., Dyer, E., Hirpa, F. & Charles, K. 2018 Climate change impact on water resources in the Awash basin, Ethiopia. *Water* **10** (11), 1560.

Taylor, K. E. 2001 Summarizing multiple aspects of model performance in a single diagram. *Journal of Geophysical Research: Atmospheres* **106** (D7), 7183–7192.

Thomas, T., Goyal, S., Goyal, V. C. & Kale, R. V. 2018 Water availability under changing climate scenario in Ur river basin. In: *Climate Change Impacts*. Springer, Singapore, pp. 213–229.

Thomson, A. M., Calvin, K. V., Smith, S. J., Kyle, G. P., Volke, A., Patel, P., Delgado-Arias, S., Bond-Lamberty, B., Wise, M. A., Clarke, L. E. & Edmonds, J. A. 2011 RCP4.5: a pathway for stabilization of radiative forcing by 2100. *Climatic Change* **109** (1–2), 77.

Toosi, A. S., Calbimonte, G. H., Nouri, H. & Alaghmand, S. 2019 River basin-scale flood hazard assessment using a modified multi-criteria decision analysis approach: a case study. *Journal of Hydrology* **574**, 660–671.

Ullah, A., Ahmad, I., Ahmad, A., Khaliq, T., Saeed, U., Habib-ur-Rahman, M., Hussain, J., Ullah, S. & Hoogenboom, G. 2019 Assessing climate change impacts on pearl millet under arid and semi-arid environments using CSM-CERES-Millet model. *Environmental Science and Pollution Research* **26** (7), 6745–6757.

Vaghefi, S. A., Keykhai, M., Jahanbakhshi, F., Sheikholeslami, J., Ahmadi, A., Yang, H. & Abbaspour, K. C. 2019 The future of extreme climate in Iran. *Scientific Reports* **9** (1), 1464.

van Vuuren, D. P., Den Elzen, M. G., Lucas, P. L., Eickhout, B., Strengers, B. J., van Ruijven, B., Wonink, S. & van Houdt, R. 2007 Stabilizing greenhouse gas concentrations at low levels: an assessment of reduction strategies and costs. *Climatic Change* **81** (2), 119–159.

van Vuuren, D. P., Stehfest, E., den Elzen, M. G., Kram, T., van Vliet, J., Deetman, S., Isaac, M., Goldewijk, K. K., Hof, A., Beltran, A. M. & Oostenrijk, R. 2011 RCP2.6: exploring the possibility to keep global mean temperature increase below 2°C. *Climatic Change* **109** (1–2), 95.

Warnatzsch, E. A. & Reay, D. S. 2019 Temperature and precipitation change in Malawi: evaluation of CORDEX-Africa climate simulations for climate change impact assessments and adaptation planning. *Science of the Total Environment* **654**, 378–392.

Wu, C. H., Huang, G. R. & Yu, H. J. 2015 Prediction of extreme floods based on CMIP5 climate models: a case study in the Beijiang River basin, South China. *Hydrology and Earth System Sciences* **19** (3), 1385–1399.

WWAP, U. 2018 *The United Nations World Water Development Report 2018: Nature-Based Solutions for Water*.

Yang, Y., Bai, L., Wang, B., Wu, J. & Fu, S. 2019 Reliability of the global climate models during 1961–1999 in arid and semiarid regions of China. *Science of the Total Environment* **667**, 271–286.

Zarghami, M., Abdi, A., Babaeian, I., Hassanzadeh, Y. & Kanani, R. 2011 Impacts of climate change on runoffs in East Azerbaijan, Iran. *Global and Planetary Change* **78** (3–4), 137–146.

Zhang, X., Wan, H., Zwiers, F. W., Hegerl, G. C. & Min, S. K. 2013 Attributing intensification of precipitation extremes to human influence. *Geophysical Research Letters* **40** (19), 5252–5257.

Zhao, T., Chen, L. & Ma, Z. 2014 Simulation of historical and projected climate change in arid and semiarid areas by CMIP5 models. *Chinese Science Bulletin* **59** (4), 412–429.

First received 13 June 2019; accepted in revised form 30 October 2019. Available online 16 January 2020